REVIEWS

Journal of Semiconductors
(2019) 40, 111604
doi: 10.1088/1674-4926/40/11/111604

Flexible and stretchable photodetectors and gas sensors for wearable healthcare based on solution-processable metal chalcogenides

Qi Yan‡, Liang Gao‡, Jiang Tang, and Huan Liu†

School of Optical and Electronic Information, Wuhan National Laboratory for Optoelectronics, Huazhong University of Science and Technology, Wuhan 430074, China

Abstract: Wearable smart sensors are considered to be the new generation of personal portable devices for health monitoring. By attaching to the skin surface, these sensors are closely related to body signals (such as heart rate, blood oxygen saturation, breath markers, etc.) and ambient signals (such as ultraviolet radiation, inflammable and explosive, toxic and harmful gases), thus providing new opportunities for human activity monitoring and personal telemedicine care. Here we focus on photodetectors and gas sensors built from metal chalcogenide, which have made great progress in recent years. Firstly, we present an overview of healthcare applications based on photodetectors and gas sensors, and discuss the requirement associated with these applications in detail. We then discuss advantages and properties of solution-processable metal chalcogenides, followed by some recent achievements in health monitoring with photodetectors and gas sensors based on metal chalcogenides. Last we present further research directions and challenges to develop an integrated wearable platform for monitoring human activity and personal healthcare.

Key words: solution-processable metal chalcogenides; gas sensor; photodetector; healthcare

Citation: Q Yan, L Gao, J Tang, and H Liu, Flexible and stretchable photodetectors and gas sensors for wearable healthcare based on solution-processable metal chalcogenides[J]. *J. Semicond.*, 2019, 40(11), 111604. http://doi.org/10.1088/1674-4926/40/11/111604

1. Introduction

In the era of artificial intelligence, high quality of life[1], environmental pollution[2] and healthcare[3] have aroused worldwide attention. These are undoubtedly closely related to human health monitoring. To meet these challenges, researchers are actively seeking solutions and new technologies to improve the level of human health monitoring[4]. Regular monitoring of vital signals helps to establish a baseline of individual health and alert users to suggest that may require further medical care[5]. Currently, regular vital signal testing is generally done using personal health monitoring systems (e.g., blood oxygen saturation monitors) which are bulky, and the systems must be set up on users to check his or her condition. This inconvenience often prevents the recording of daily health statistics[6]. Recently, wearable electronic devices have attracted great attention due to their long-term human health monitoring capabilities. Physical, chemical, biological and environmental conditions can be monitored by employing varieties of efficient and flexible sensors, thereby reducing human discomfort[7–11]. Flexible wearable electronic sensors may be connected to clothes or even installed directly on human skin to monitor human activities in a remote but more timely manner compared to traditional diagnostic and medical device[12]. Flexible wearable electronic sensing devices will transform traditional diagnostic and medical device innovation through portable, remote and timely ways[13].

As one of the potential wearable electronic devices, photodetector and gas sensor play an indispensable role in health monitoring system, such as forecasting alarm and pre-diagnosis by tracking specific signals in the environment or from human body. Owing to their unique properties like electronic conduction and energy bandgap which are highly programmable via a low-temperature processing route, solution-processable metal chalcogenides emerge as ideal building blocks for flexible and stretchable photodetectors and gas sensors. The merits of metal chalcogenides are high sensitivity and mild preparation in the smart sensor application. Sensing response/sensitivity is the ratio of signal to noise. However, their demerit is low stability. Herein we reviewed the recent progress of flexible and stretchable sensors for wearable healthcare based on solution-processable metal chalcogenides.

2. Requirements of healthcare monitoring with photodetectors and gas sensors

2.1. Photodetectors for healthcare monitoring

Sensors are the main way and means for humans to obtain information in the natural and artificial fields. They are the basic devices of Internet of Things that promote the acceleration of digital and network to intelligence. As one of physical sensors, photodetectors can detect light simply through the change of materials conductivity upon radiation.

Qi Yan and Liang Gao contribute equally.
Correspondence to: H Liu, Huan@hust.edu.cn
Received 30 JULY 2019; Revised 19 OCTOBER 2019.

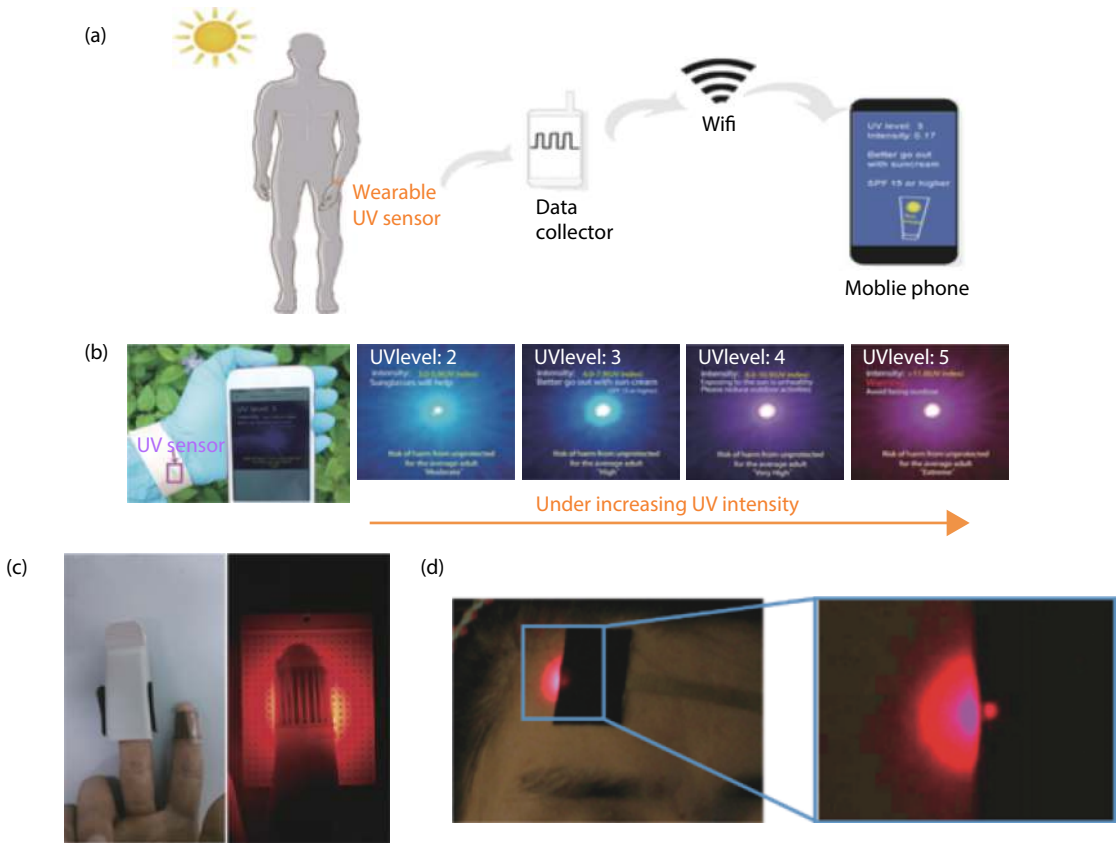

Fig. 1. (Color online) Photodetectors for healthcare monitoring. (a) Schematic illustration of the wearable photodetector as a real-time UV monitor[14]. Copyright 2018, Adv Mater. (b) Photographs of a wearable real-time UV sensor in real life[14]. Copyright 2018, Adv Mater. (c) Comparison between traditional heart-rate sensor probe (clipped at middle finger) and the wearable photodetector (worn at forefinger)[15]. Copyright 2014, Appl Phys Lett. (d) Image of a device laminated on the skin of forehead, with an operating m-ILED (wavelength 650 nm) under room light illumination and in the dark[16]. Copyright 2014, Nat Commun.

In the field of health monitoring, photodetectors for ultraviolet radiation monitoring[14] (Figs. 1(a) and 1(b)), heart rate monitoring[15] (Fig. 1(c)) and blood oxygen saturation monitoring[16] (Fig. 1(d)) have been demonstrated very promising for practical application.

The ultraviolet rays by the sun are the main source of ultraviolet radiation in our daily life. Excessive ultraviolet radiation can cause skin wrinkles, aging and relaxation. In addition, ultraviolet radiation is also considered as the main cause of skin cancer[16]. Ultraviolet light is a general term for the wavelength of light in the electromagnetic spectrum of 10–400 nm. According to the wavelength classification, ultraviolet light can be divided into three types: UV-A (320–400 nm), UV-B (280–320 nm), UV-C (100–280 nm)[17]. Among them, UV-A is associated with long-term damage of skin cells, and UV-B causes direct damage to skin cells and causes skin cancer. UV-C with higher energy cannot reach earth surface due to barrier of ozone layer[18]. Therefore, there is great need for intelligent and highly sensitive photodetectors to monitor ultraviolet radiation (especially UV-A and UV-B) in real time and remind human to prevent excessive exposure to ultraviolet light.

Heart rate, a direct signal of heart health, can reflect person's blood circulation status. Heart rate detection, an irreplaceable medical physiological indicator in clinical medicine, occupies an extremely important position in body monitoring. Studies have shown that increased heart rate is one of the major risk factors for death of patients with cardiovascular disease[19]. For people at high risk of cardiovascular disease, long-term continuous monitoring of heart rate is necessary to establish the first line of defense. Through continuous and accurate ECG monitoring and analysis, timely detection of abnormal cardiac performance could obtain valuable visits and intervention time for patients. For another example, heart rate monitoring ensures that athletes are trained at normal training intensity, objectively assessing physical activity and energy expenditure levels[20] and preventing overtraining[21]. Therefore, there is a need for high performance photodetectors that can monitor the heart rate of human body in real time.

Photodetectors used for the blood oxygen saturation monitoring have been demonstrated. Oxygen saturation is the ratio between the concentration of oxygenated (HbO_2) hemoglobin and deoxygenated (Hb) hemoglobin. The saturation of blood oxygen is an important physiological parameter reflecting the function of breathing and circulation. The oxygen saturation value SvO_2 in venous blood is of important clinical significance, related to the flow of blood to blood tissue and its metabolic rate[22]. In addition, the therapeutic effect can be followed up by detecting blood oxygen. Blood oxygen monitoring is desperately needed in the conditions of first aid and transshipment, fire emergency, and high altitude flight. In outdoor activities, monitoring blood oxygen saturation can assess the physical condition in real time and ad-

just the current strength. Therefore, the use of photodetectors for real-time monitoring of human blood oxygen saturation is of great significance.

2.2. Gas sensors for healthcare monitoring

The safety and quality of human life are closely related to the gas environment. Gas sensor is one of the most effective ways for real-time monitoring and disaster warning of flammable, explosive and toxic gases in real time[23]. Therefore, gas sensors are of a major need in the field of health monitoring. Exemplary and emerging applications of gas sensors are summarized, including industrial safety (such as CO_2, CO, O_3, H_2S, NH_3, NO_x, SO_2, CH_4, industrial smog and waste odor), environmental monitoring (such as NO_2, SO_2, CO_2, O_3), safety alarms (such as natural gas, liquefied petroleum gas, gas), health diagnostics (such as NH_3, acetone, VOCs) and other application scenarios.

With the development of the petrochemical industry, the types and applications of flammable, explosive, and toxic gases have increased. The leakage of these gases in the process of production, transportation and use could lead poisoning, fire and even explosion accidents, seriously endangering people's lives. In the event of a gas leak, appropriate measurement must be taken as soon as possible to reduce the accident loss to a lower level. This puts high demands on gas detection and monitoring equipment. The development of gas sensors makes them more and more widely used in industrial safety. The environmental problems also have great influence on our daily life. For example, as one of the toxic and harmful gases, NO_2 is one of the main harmful gases released from automobile exhaust and fossil fuel combustion. This pollution not only causes serious respiratory problems in humans, such as pulmonary edema, but also threatens animals, plants and the environment[23, 24]. SO_2 is another common air pollutant and one of the causative factors that causes damage to vegetation and materials[25]. An increase in CO_2[26] concentration causes greenhouse effect, which leads irreversible climate change. Monitoring of these gases is becoming a priority area for human health[27–30].

In the fields of domestic gas leakage, coal mine safety, oil exploration, etc., gas sensors are of major need as safety alarms. Because of its high calorific value, natural gas, a widely used fuel, produces less smoke and does not cause much damage to the environment. However, it has serious leakage risks, which may cause an explosion. Inhalation of the human body may also cause suffocation[31]. When the gas content in the air is 5% to 16%, it will cause an explosion when it encounters fire, which seriously threatens people's lives. Oil exploration also has the threat of flammable gas. Therefore, the importance of gas sensors in the field of safety alarms is self-evident. Moreover, part of the body's metabolic products can be transported to the lungs via the blood and enter the exhaled gas by gas exchange into the alveoli. In recent years, exhaled gas detection has received increasing attention as a means of understanding the physiological metabolic processes and disease states of humans. It is a non-invasive disease diagnosis that compares to the concentration of respiratory biomarkers in healthy people to determine health status[32].

Table 1 lists some of the gas markers used for respiratory testing, which can reflect certain physiological and pathological conditions of human body. Olopade *et al.*[33] reported that in acute asthma patients, the content of pentane in the exhaled breath was significantly higher than the normal population. Another study confirmed that the pentane content would follow the acute myocardium changes in the formation of infarction[34]. Salerno-Kennedy described the association of isoprene with cancer in his review[35]. Dong *et al.*[36] reported that patients with diabetes were of significantly higher levels of acetone in their exhaled breath. The presence of nitric oxide in the breath above 50 ppb could indicate respiratory inflammation[32], such as asthma attacks. Ammonia is in the ppb range in exhaled gases of healthy individuals, but for people with kidney disease or failure, ammonia exhaled concentrations can reach the ppm range[37].

Table 1. Respiratory gas markers and pathology.

Exhaled gas marker	Illness	Reference
Pentane	Acute asthma, acute myocardial infarction	[33, 34]
Isoprene	Cancer	[35]
Acetone	Diabetes	[36]
NO_x	Lung inflammation	[37]
NH_3	Kidney disease or ulcer	[38]

3. Solution-processed metal chalcogenides

In recent years, metal chalcogenides have been widely used in flexible wearable electronic devices. Common metal chalcogenides include PbS, PbSe, CdS, CdSe, HgTe, MoS_2, Bi_2S_3 and so on. These materials could be synthesized by solution process. In the solution synthesis system, the solution and surfactant are reasonably selected based on different target metal chalcogenides, and the nucleation and growth process of the product can be controlled by adjusting parameters such as reaction temperature and reaction time[39]. In addition, the solution method does not involve severe reaction conditions (e.g., high temperature, high pressure) and a large number of products, thus avoiding material deactivation, deterioration or even degradation of material properties due to the collapse of nanostructures.

3.1. Solution-processed synthesis

The widespread use of metal chalcogenides has benefited from the synthesis of nanostructured materials of different sizes and new forms. When the size of metal chalcogenides is reduced to the nanometer scale, new physical and chemical properties occur in well-known quantum size effects[40]. In addition, nanostructured metal chalcogenides provide greater specific surface area[41, 42]. In Table 2, we summarize some solution-processed metal chalcogenides.

Quite a few journals have been published on the synthesis of metal chalcogenides with nanostructures. Liu *et al.*[30] synthesized ultra-small PbS QDs by thermal injection and sprayed them on alumina substrate at room temperature. Fig. 2(a) clearly shows PbS QDs with uniform distribution and approximately spherical particles, and the surface spacing of 0.343 and 0.297 nm corresponds to (111) and (200) crystal surfaces, respectively. Franky *et al.*[43] synthesized PbSe nanocrystals in solution for near infrared photodetectors. Fig. 2(b) shows that the absorption spectrum can be adjusted to a wide wavelength range of 1800 nm by changing the grain size of PbSe. Jena *et al.*[44] used solution–liquid–solid (SLS)[45]

Table 2. Methods of synthesis of some metal chalcogenides.

Materials	Morphology structure	Synthetic method	Reference
PbS	QDs	Hot-injection method	[30]
PbS	QDs	Cation exchange method	[61]
PbSe	Nanocrystalline	Solution method	[43]
CdSe	Nanowires	Solution-Liquid-Solid method	[44]
CdSe–CdS	Core-shell QDs	Solution method	[62]
Bi_2S_3	Nanorods	Solution method	[46]
Bi_2S_3	Nanobelts	Hydrothermal method	[63]
HgTe	QDs	Solution method	[47]
ZnS	Nanocrystalline	Solution method	[48]
ZnS	Nanowires	Solvent hot method	[64]
Ag_2Se	Nanowires	Solution method	[49]
Ag_2Se	Nanocrystalline	Cation exchange method	[65]
Fe_7S_8	Nanocrystalline	Single-source precursor method	[66]
MoS_2	Nanosheets	Liquid exfoliation method	[59]
WS_2	Nanosheets	Liquid exfoliation method	[59]
WS_2	Nanosheets	Sulfidation-induced method	[61]

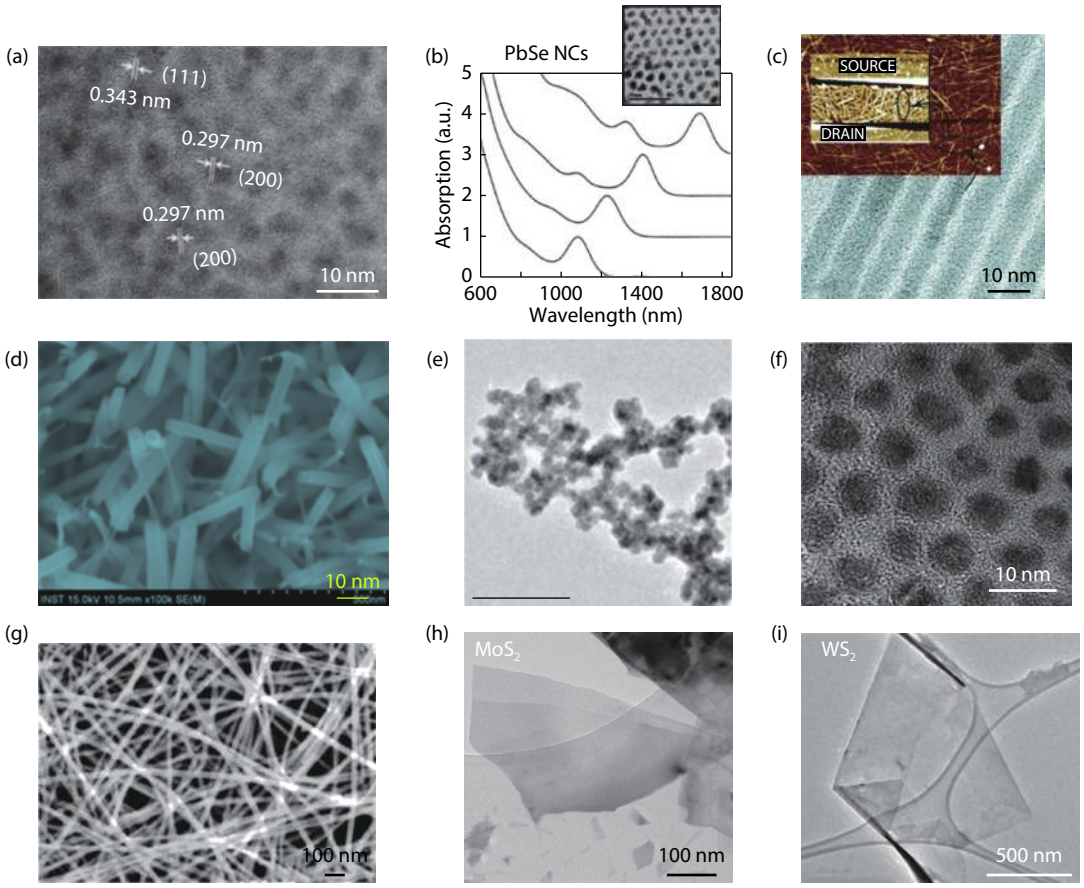

Fig. 2. (Color online) Some solution-processed metal chalcogenides. (a) HRTEM of PbS CQDs[30]. Copyright 2016, Thin Solid Films. (b) Typical absorption spectra of PbSe Nanocrystal from different sizes and TEM image of PbSe[43]. Copyright 2011, Adv Funct Mater. (c) TEM image of solution-synthesized CdSe NWs, with (inset) an AFM image of a network of such NWs formed on a SiO_2/Si substrate[44]. Copyright 2007, Nano Lett. (d) SEM images of Bi_2S_3 Nanorods[46]. Copyright 2017, J Photochem Photobiol A. (e) TEM image of HgTe CQDs with an absorption onset at 5 mm. Scale bar, 100 nm[47]. Copyright 2011, Nature Photonics. (f) TEM image of 5 nm quasi-spherical ZnS nanocrystals[48]. Copyright 2005, J Am Chem Soc. (g) SEM of Ag_2Se[49]. Copyright 2001, J Am Chem Soc. (h) TEM of MoS_2 nanosheets[59]. Copyright 2011, Science. (i) TEM of WS_2 nanosheets[59]. Copyright 2011, Science.

method to grow CdSe nanowires (Fig. 2(c)). The benefits of using SLS include: higher CdSe nanowire yield, lower synthesis temperature (< 400 °C) and prevention of potential oxide formation. Kim *et al.*[46] successfully prepared Bi_2S_3 thin film from bismuth chloride and thioacetamide solution by solution treatment method and provided a convenient, economical and large-scale method for the production of Bi_2S_3 nanorods as shown in Fig. 2(d). Philippe *et al.*[47] synthesized HgTe QDs by solution method (Fig. 2(e)). The final particle size of HgTe depends on the flask temperature when the Hg precurs-

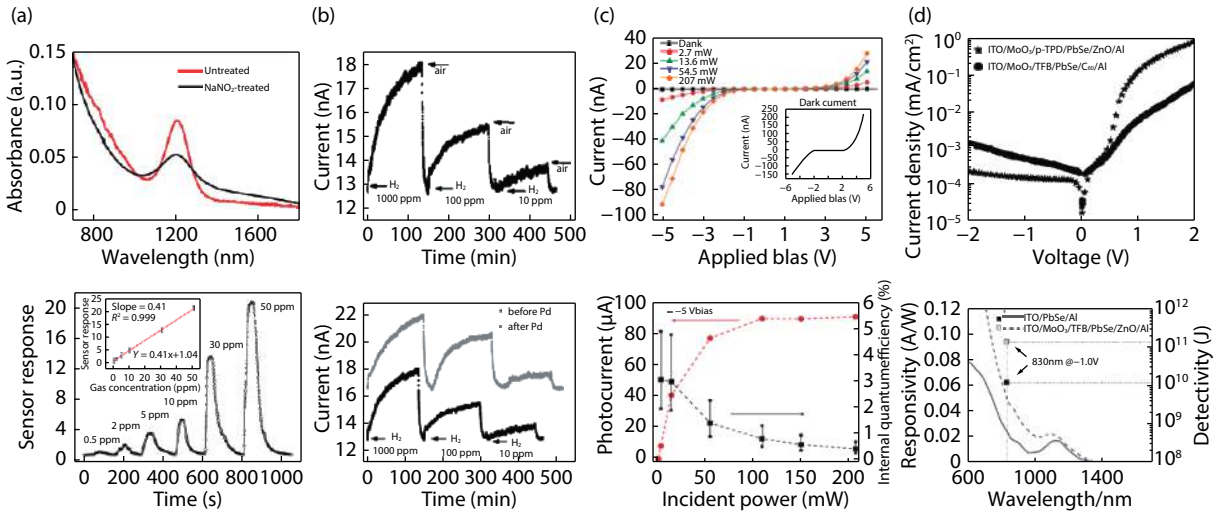

Fig. 3. (Color online) (a) Absorption spectra of PbS CQD film and response curves of the sensor to NO_2 of different concentrations[30, 67]. Copyright 2014, Adv Mater. (b) Performance of Bi_2S_3 nanowire sensor[68]. Copyright 2008, J Phys Chem. (c) PbS QDs infrared photodetectors and photovoltaics[70]. Copyright 2005, Nat Mater. (d) Dark current-voltage, responsivity and measured detectivity characteristics of PbSe nanocrystal photodetectors[43]. Copyright 2011, Adv Funct Mater.

or is injected. As the reaction temperature increases, the reaction rate increases and the final product particles are larger. Taeghwan *et al.*[48] synthesized quantum-sized ZnS nanocrystals with quasi-spherical and nanorod shapes through an aging reaction mixture containing diethyl zinc, sulfur, and amine (Fig. 2(f)). Xia *et al.*[49] first reported that the single crystal Ag_2Se nanowires were obtained by the reaction of triangle Se (t-Se) nanowires with $AgNO_3$ solution at room temperature (Fig. 2(g)). This template reaction can spread to other synthesis systems.

In addition, 2D transition metal sulfides (TMDs) because of the special band structure, semiconductor or superconducting properties and excellent mechanical properties[50–56]. TMD consists of a hexagon metallic atom layer (M) and a chalcogen atom (X) sandwiched between two layers of chalcogen atoms (MX_2). Although the bonding within these three layers is covalent, adjacent sheets are stacked on top of each other through van der Waals interactions to form 3D crystals. TMD occurs in more than 40 different types[57, 58], depending on the combination of chalcogen (S, Se, or Te) and transition metals (Mo, W, etc.). Jonathan *et al.*[59] dispersed the layered compounds of MoS_2, WS_2 effectively in ordinary solvents by using a liquid exfoliation method and scaled up the test dose to synthesize a large number of materials (Figs. 2(h) and 2(i)). Cheon *et al.*[60] reported a vulcanization-induced shape transformation process by using one-dimensional $W_{18}O_{49}$ nanorods to manufacture 2D WS_2 nanocrystals. The obtained single 2D WS_2 nanocrystals can be further assembled by van der Waals force to form multilayer superimposed nanocrystals. However, limited by the size of nanorods, the lateral size of WS_2 nanocrystals is less than 100 nm.

3.2. Gas-sensitive and photon-sensitive characteristics

Several metal chalcogenide compounds have been selected for analysis of their properties, including photoelectric and gas-sensitive properties. Liu *et al.*[30, 67] synthesized PbS QDs by solution method and successfully removed the surface oleic acid long chain ligands by sodium nitrite inorganic salt solution at room temperature, enhancing the gas adsorption activity of QDs. Through controlling synthesis of PbS QDs, sulfur vacancy increased, and active sites for gas adsorption further increased. Highly sensitive NO_2 gas sensor was designed and prepared at room temperature. As shown in Fig. 3(a), six groups of tests were carried out at the concentration of NO_2 at 0.5, 2, 5, 10, 30, and 50 ppm, respectively. The sensor response was approximately linearly dependent on the concentration of NO_2 gas within the range of 0.5 to 50 ppm, and the lowest limitation of theoretical detection was measured at 84 ppb. The response and recovery time of the sensor were 4 and 52 s (on the PET substrate) respectively, which was the highest level of the NO_2 room temperature gas sensor at that time.

Chen *et al.*[68] synthesized Bi_2S_3 nanowires by hydrothermal method and deposited Pt electrodes on a single Bi_2S_3 nanowire. The sensor has excellent H_2 sensing performance and can detect H_2 at 10 ppm at room temperature (in N_2 atmosphere) with a sensitivity of 22% (Fig. 3(b)). The sensing mechanism of Bi_2S_3 nanowires is mainly due to the increase of electron density, mobility caused by H_2, and the diffusion of H_2 into nanowires. Meanwhile, Pd surface modification on Bi_2S_3 nanowires further improves the sensor performance.

Jin *et al.*[69] synthesized MoS_2 nanosheet and Pd nanoparticle composite by solution method for H_2 detection at room temperature. The response of the prepared MoS_2-Pd composite sensor is about 10 (for 50 000 ppm H_2), and the response and recovery time are 40 and 83 s respectively. Compared with pure MoS_2 sensors, Pd-doped MoS_2 composite sensors rely on Pd's catalytic effect on H_2 to obtain higher sensitivity and faster response/recovery time. Recovery time was further reduced to 28 s by increasing annealing time.

Sargent *et al.*[70] synthesized PbS QDs by solution method, and the synthesized PbS QDs can adjust the absorption peak in the range of 800–2000 nm. As shown in Fig. 3(c), the internal quantum efficiency of PbS QDs photodetector is 3%, the switching ratio (the ratio of photocurrent to dark current) is 630, and the maximum response is 3.1×10^{-3} A/W under the irradiation of −5 V bias voltage and 975 nm laser. The photovoltaic response excited at 975 nm results in a maxim-

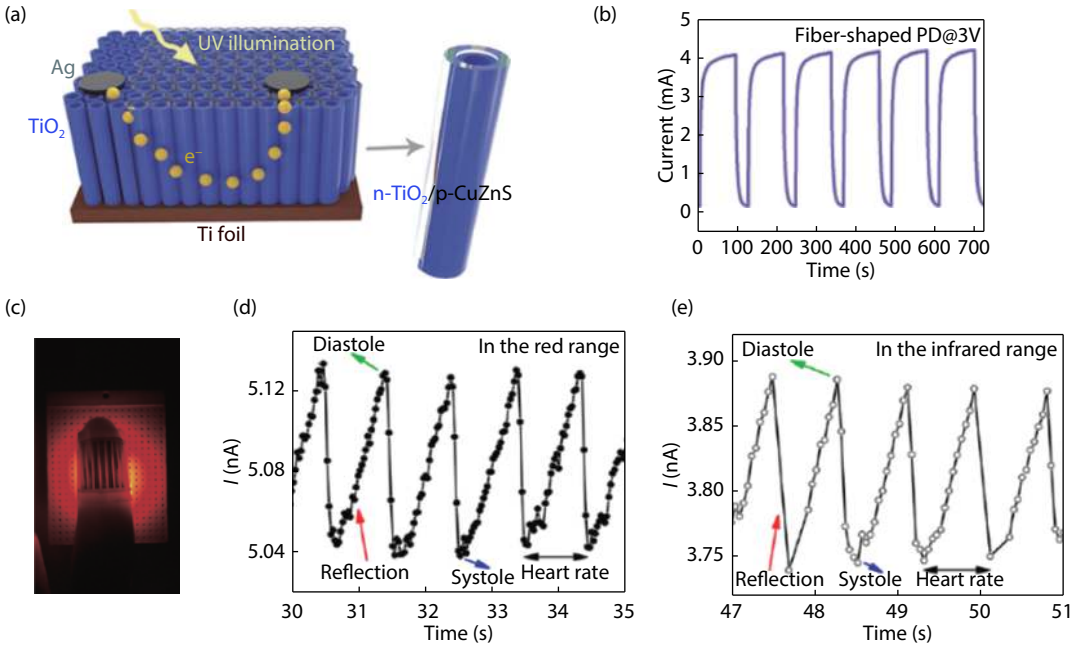

Fig. 4. (Color online) (a) Schematic diagram of the device configuration of p-CuZnS/n-TiO_2 NTAs with Ag contacts[14]. Copyright 2018, Adv Mater. (b) The on–off switching tests of the fiber-shaped PD at 3 V under 350 nm[14]. Copyright 2018, Adv Mater. (c) Heart-rate test of the PbS QD PDs under red LEDs[15]. Copyright 2014, Appl Phys Lett. (d) and (e) The original heart-rate signal measured through the CAB PDs in the red and infrared spectral ranges[15]. Copyright 2014, Appl Phys Lett.

um open circuit voltage of 0.36 V, a short-circuit current of 350 nA, and an external quantum efficiency of 0.006%. Compared with other results, the internal quantum efficiency of PbS QD infrared photoconductive detector improves by three orders of magnitude, and the infrared photovoltaic effect of this material is observed for the first time.

Franky *et al.*[43] synthesized PbSe nanocrystals by solution method. It is found that poly[(9,9 '-dioctylfluorenyl-2,7-diyl)-co -(4,4'-(N-(4-sec-)diphenylamine)] (TFB) and ZnO, respectively as the electronic barrier layer and cavity barrier layer of PbSe infrared photodetectors, can significantly reduce the dark current of photodetectors under reverse bias as shown in Fig. 3(d). Thereby, the detectivity of the devices is improved up to 10^{12} J. At the same time, it is found that ZnO, as a hole barrier layer of PbSe infrared photodetector, can effectively increase the stability of the device.

4. Device performance based on metal chalcogenides

4.1. Photodetectors performance

At present, metal chalcogenides have been reported as photodetector materials for ultraviolet and heart rate monitoring. Fang *et al.*[14] developed a new self-powered p-CuZnS/n-TiO_2 ultraviolet photodetector with high performance. The device structure is shown in Fig. 4(a), including titanium foil, p-CuZnS/n-TiO_2 and silver electrode from bottom to top. Photodetector has a responsivity of 2.54 mA/W to 300 nm UV light at 0 V bias. In addition, by replacing titanium foil with thin titanium wire for anodizing treatment, the traditional flat rigid device is cleverly transformed into a fibrous flexible and wearable device. The fibrous device displays a responsivity of 640 A/W, an external quantum efficiency of 2.3×10^3, and a photocurrent of 4 mA at 3 V bias (Fig. 4(b)). This flexible wearable UV photodetector could be used in practical applications to prevent UV harm on skin. The device's high sensitivity and light response make it easy to integrate into a commercial data collector that can not only record the real-time UV intensity generated by the photocurrent, but also transmit the data to our smartphones via Wi-Fi. Finally, the wearable UV photodetector can be worn on the wrist to monitor the UV radiation in the surrounding environment in real time. Wi-Fi transmits the monitoring data to the smartphone and grades the UV intensity of the surroundings. This provides an effective, practical and convenient way to protect UV alarms from excessive exposure.

Based on PbS QDs and multi-walled carbon nanotube hybrid film materials, wearable photodetectors designed by Gao *et al.*[15] can be used for heart rate detection (Fig. 4(c)). Based on the high sensitivity of PbS QDs and conductive and mechanical properties of MWCNTs, the photodetector shows responsivity and detectivity of 583 mA/W and 3.25×10^{12} J, and can bear a large number of cycle (at least 10 000 times) and wide angle bending (up to 80 times). In addition, wearable PbS QDs photodetectors are used to measure heart rates in the infrared and near infrared (NIR) range. The output signal can clearly show the patients' heart rate change. Measurements in red (Fig. 4(d)) and infrared (Fig. 4(e)) clearly show pulse characteristics including heart rate, systole, diastole, and pulse wave reflection. Compared with traditional heart rate sensor, PbS QDs/MWCNT photodetectors have smaller size, superior photoelectric performance and wider response spectrum. In the future, there will be better development and application prospects in the field of health monitoring (heart rate).

4.2. Gas sensors performance

Gas sensor has been widely used in flammable, explosive, toxic and harmful gas detection, environmental monitoring, security alarm and other fields as an indispensable part.

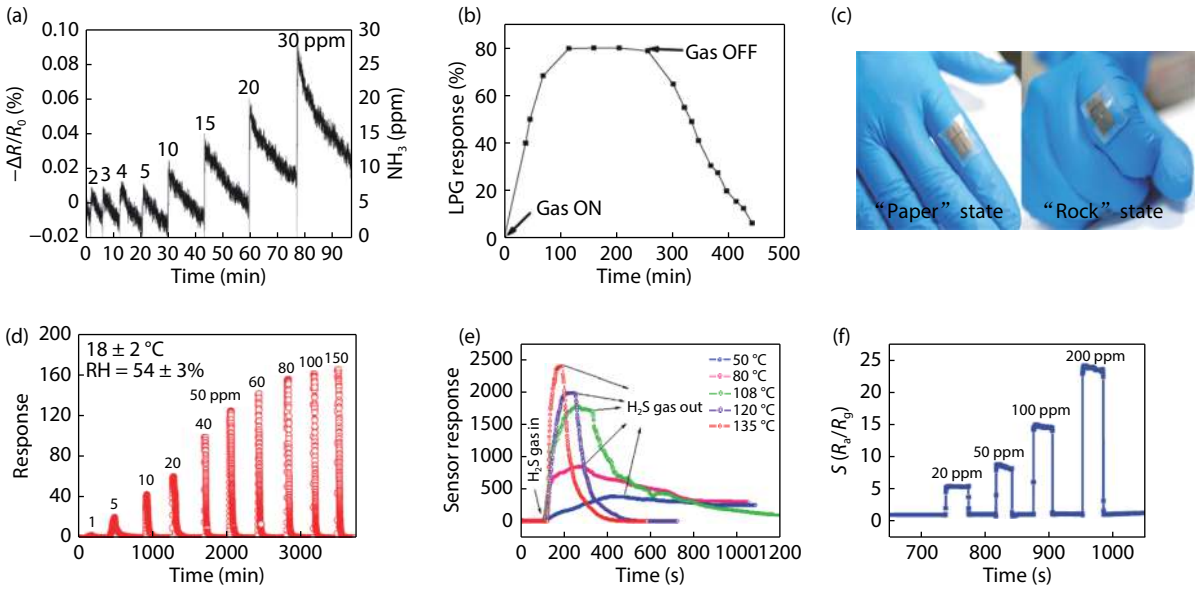

Fig. 5. (Color online) (a) Sensor response plots show percentile resistance change versus time of the MoS_2 film with a bias voltage of 0.5 V, upon consequent NH_3 exposures from 2 to 30 ppm[71]. Copyright 2013, Adv Mater. (b) Gas response (%) versus time of n-CdS/p-polyaniline heterojunction at a fixed voltage of 2 V and at a concentration of 1040 ppm LPG[72]. Copyright 2010, Sens Actuators B. (c) Gas sensor device attached on the finger joint with "paper" and "rock" state[73]. Copyright 2018, ACS Sensors. (d) Real-time sensing curves and sense response toward different concentrations of NO_2 at room temperature[73]. Copyright 2018, ACS Sensors. (e) Response curves toward 50 ppm of H_2S of the sensor at different temperatures[74]. Copyright 2015, Sens Actuators B. (f) Response–recovery curves of the gas sensor towards 20, 50, 100, and 200 ppm ethanol, respectively[75]. Copyright 2014, RSC Adv.

Different materials can be used according to different gas detection objects. Duesberg *et al.*[71] proposed the gas-phase growth of MoS_2 film by chemical vapor deposition (CVD) and studied its performance as a gas sensor to detect NH_3. CVD produces highly uniform and structured MoS_2 patterns that can be directly contacted by electrodes deposited by a shadow mask. The thickness of MoS_2 film can be changed by changing the thickness of pre-deposited Mo layer. Fig. 5(a) shows the response curve of the MoS_2 gas sensor for 2 to 30 ppm NH_3 gas concentrations (the bias is 0.5 V). Since NH_3 is an electronic conductor, it has n-doped properties. When a MoS_2 film is exposed to NH_3 in the gaseous state, the MoS_2 surface of the adsorbent molecule moves the Fermi energy level to the conduction band, resulting in a reduction in resistance. The MoS_2 gas sensor has a response recovery time of 15 s, but it cannot be immediately restored at room temperature, requiring additional thermal assistance. And its detection limit theoretically reaches 300 ppb. MoS_2 gas sensor has the advantages of fast response, high sensitivity and low detection limit. Lokhande *et al.*[72] manufactured a liquefied petroleum gas (LPG) sensor based on n-CdS/polyaniline heterojunction film using a simple and inexpensive electrodeposition technique. As shown in Fig. 5(b), when the gas sensor targets at 1040 ppm LPG at fixed voltage of 2 V, the maximum gas response can reach 80%, and the response and recovery time are 105 and 165 s respectively. N-CdS/polyaniline heterojunction films showed rapid response and recovery characteristics, and high stability to LPG at room temperature. Song *et al.*[73] demonstrated the first fully stretchable gas sensor, which operated at room temperature with high moisture resistance stability. They created a crumpled PbS QD sensing layer on an elastomer substrate with flexible graphene as the electrode. The stretchable gas sensor showed great response to NO_2 at room temperature, good tensile properties and good deformation. By controlling the prestrain of the flexible substrate, the NO_2 response was improved by 5.8 times at room temperature, and the ideal tensile property was achieved even under 1000 times of tensile/relaxation cycle deformation (Fig. 5(c)). The uniform wavy structure of the crumpled QD gas sensitive layer could improve the resistance to moisture interference. The sensor response increased with the increase of NO_2 gas concentration, with a saturation trend in the range of 1–150 ppm (Fig. 5(d)). Li *et al.*[74] demonstrated a highly sensitive and selective H_2S gas sensor based on PbS QDs. Sensor resistance decreases with H_2S gas exposure. As the operating temperature increases in the range of 50–135 °C, the sensor response increases, while the response and recovery time decreases. When detecting 50 ppm H_2S gas, the sensor can fully recover at 108 °C and obtain the highest response of 2389 at 135 °C (Fig. 5(e)), with response and recovery time of 54 and 237 s respectively. The dependence of sensor response on H_2S gas concentration in the range of 10–50 ppm is linear. When the temperature is 135 °C, the theoretical detection limit can be calculated to be 17 ppb, and it has a good selectivity to H_2S gas at the rising temperature (little cross sensitivity to SO_2, NO_2 and NH_3). Chen *et al.*[75] synthesized one-dimensional single crystal CdS nanowires by solvent thermal method and used them as active nanomaterial to detect ethanol. For the detection of 100 ppm ethanol, the response and recovery time of the sensor were 0.4 and 0.2 s respectively, much faster than the previously reported. The sensor has good selectivity to ethanol, little cross-sensitivity to methanol, formaldehyde, acetone, hydrogen sulfide, ammonia, carbon monoxide, and benzene. Fig. 5(f) shows the recovery curve of the gas sensor response to different concentrations of ethanol (20, 50, 100, and 200 ppm). The response

of the gas sensor increases with the increase of ethanol concentration.

5. Conclusion

In this review, we highlight the need of wearable photodetectors and gas sensors for health monitoring in real time. Flexible and stretchable wearable electronic devices have new requirements on sensitive materials, including flexibility, stretchability, high mechanical properties and high electrical conductivity. We listed the reported materials used in wearable electronic devices and analyzed their properties. We further proposed the advantages of metal chalcogenides synthesized by solution method, and summarized the synthesis methods, morphology, photoelectric and gas-sensitive characteristics of some metal chalcogenides at present. Finally, some photodetectors and gas sensors based on metal chalcogenides which have been used for health monitoring (including ultraviolet radiation, heart rate, toxic and harmful gases, flammable and explosive gases, etc.) were listed and their performance was analyzed.

There is an urgent need on flexible, stretchable wearable electronic devices to monitor human activities and personal health care. However, due to the limitation of materials, the current wearable electronic devices can't meet all the requirements of practical application. Therefore, the preparation of highly sensitive wearable electronic devices is still the main potential of future research. In addition, the integration of wearable electronic devices with other platforms, such as data storage, data transmission system can further play a huge role on monitoring human activities and personal health care. But integrating multiple functional components into wearable electronics is also a considerable challenge.

Acknowledgments

This work in this paper was supported by National Natural Science Foundation of China (61861136004) and the National Key R&D Program of China (2016YFB0402705). H. Liu acknowledges the Innovation Fund of WNLO, and Program for HUST Academic Frontier Youth Team (2018QYTD06).

References

[1] Gary L A, Patrick J D. The disability paradox: high quality of life against all odds. Soc Sci Med, 1999, 48, 977
[2] Ren X, Chen C, Masaaki N, et al. Carbon nanotubes as adsorbents in environmental pollution management: a review. Chem Eng J, 2011, 170, 395
[3] Ashraf D, Aboul E H. Wearable and implantable wireless sensor network solutions for healthcare monitoring. Sensors, 2011, 11, 5561
[4] Zheng Y L, Ding X R, Carmen C Y P, et al. Unobtrusive sensing and wearable devices for health informatics. IEEE Trans Biomed Eng, 2014, 61, 1538
[5] Yasser K, Aminy E O, Claire M L, et al. Monitoring of vital signs with flexible and wearable medical devices. Adv Mater, 2016, 28, 4373
[6] Jaemin K, Mincheol L, Hyung J S, et al. Stretchable silicon nanoribbon electronics for skin prosthesis. Nat Commun, 2014, 5, 5747
[7] Joshua R W, Joseph W. Wearable electrochemical sensors and biosensors: a review. Electroanalysis, 2013, 25, 29
[8] Li L, Lou Z, Chen D, et al. Recent advances in flexible/stretchable supercapacitors for wearable electronics. Small, 2018, 14, 1702829
[9] Lou Z, Wang L, Shen G. Recent advances in smart wearable sensing systems. Adv Mater Technol, 2018, 3, 1800444
[10] Webb R C, Bonifas A P, Behnaz A, et al. Ultrathin conformal devices for precise and continuous thermal characterization of human skin. Nat Mater, 2013, 12, 938
[11] Wang X, Gu Y, Xiong Z, et al. Electronic skin: silk-molded flexible, ultrasensitive, and highly stable electronic skin for monitoring human physiological signals. Adv Mater, 2014, 26, 1336
[12] Morteza A, Aekachan P, Sangjun L, et al. Highly stretchable and sensitive strain sensor based on silver nanowire–elastomer nanocomposite. ACS Nano, 2014, 8, 5154
[13] Wang X, Liu Z, Zhang T. Flexible sensing electronics for wearable/attachable health monitoring. Small, 2017, 13, 1602790
[14] Xu X, Chen J, Cai S, et al. A real-time wearable UV-radiation monitor based on a high-performance p-CuZnS/n-TiO_2 photodetector. Adv Mater, 2018, 30, 1803165
[15] Gao L, Dong D, He J, et al. Wearable and sensitive heart-rate detectors based on PbS QDs and multiwalled carbon nanotube blend film. Appl Phys Lett, 2014, 105, 153702
[16] Setlow R B. The wavelengths in sunlight effective in producing skin cancer: a theoretical analysis. Proc Natl Acad Sci, 1974, 71, 3363
[17] Saraiya M, Glanz K, Briss P A, et al. Interventions to prevent skin cancer by reducing exposure to ultraviolet radiations: a systematic review. Am J Preven Med, 2004, 27, 422
[18] Narayanan D L, Saladi R N, Fox J L. Ultraviolet radiation and skin cancer. Int J Dermat, 2010, 49, 978
[19] Palo P, Lutgarde T, Jan A S, et al. Predictive value of clinic and ambulatory heart rate formortality in elderly subjects with systolic hypertension. Arch Inter Med, 2002, 162, 2313
[20] Keytel R, Goedecke H, Noakes D, et al. Prediction of energy expenditure from heart rate monitoring during submaximal exercise. J Sports Sci, 2005, 23, 289
[21] Achten J, Jeukendrup E. Heart rate monitoring, applications and limitations. Sports Med, 2003, 33, 517
[22] Hamootal D, Meir N, Dror F. Simulation of oxygen saturation measurement in a single blood vein. Opt Lett, 2016, 41, 4312
[23] Liu H, Li M, Oleksandr V, et al. Physically flexible, rapid-response gas sensor based on colloidal QDs solids. Adv Mater, 2014, 26, 2718
[24] Li M, Zhang W, Shao G, et al. Sensitive NO_2 gas sensors employing spray-coated QDs. Thin Solid Films, 2016, 618, 271
[25] Paul U, William H S. SO_2 in the atmosphere: a wealth of monitoring data, but few reaction rate studies. ACS Publications, 1969
[26] Michal S, Inigo G, Reto P, et al. A simple and fast electrochemical CO_2 sensor based on $Li_7La_3Zr_2O_{12}$ for environmental monitoring. Adv Mater, 2018, 30, 1804098
[27] Zimmerling R, Dammgen U, Kusters A, et al. Response of a grassland ecosystem to air pollutants. IV. the chemical climate: concentrations of relevant non-criteria pollutants (trace gases and aerosols). Environ Pollut, 1996, 91, 139
[28] Odlyha M, Foster G. M, Cohen N. S, et al Microclimate monitoring of indoor environments using piezoelectric quartz crystal humidity sensors. J Environ Monit, 2000, 2, 127
[29] Emil J B. Indoor pollution and its impact on respiratory health. Annals of Allergt Asthma and Immunology, 2001, 87, 33
[30] Becker T, Muhlberger S, Bosch-von Braunmuhl C, et al. Air pollution monitoring using tin-oxide-based microreactor systems. Sens Actuators B, 2000, 69, 108
[31] Rajitha S, Swapna T. A security alert system using GSM for gas leakage. Int J VLSI Embed Syst, 2012, 03, 173
[32] James E E, Alexander S. Carbon nanotube based gas sensors toward breath analysis. ChemPlusChem, 2016, 81, 1248
[33] Christopher O O, Mohamed Z, William I S, et al. Exhaled pentane levels in acute asthma. Chest, 1997, 111, 862

[34] Zeev W W, Alan J B, Paul A S, et al. High breath pentane concentrations during acute myocardial infarction. Lancet, 1991, 337, 933
[35] Rossana S K, Kevin D C. Potential applications of breath isoprene as a biomarker in modern medicine: a concise overview. Wien Klin Wochenschr, 2005, 117, 180
[36] Dong L, Shen X, Deng C. Development of gas chromatography–mass spectrometry following headspace single-drop microextraction and simultaneous derivatization for fast determination of the diabetes biomarker, acetone in human blood samples. Analyt Chim Acta, 2006, 569, 91
[37] Hçgman M, Holmkvist T, Wegener T, et al. Extended NO analysis applied to patients with COPD, allergic asthma and allergic rhinitis. Respir Med, 2002, 96, 24
[38] Di N C, Paolesse R, Martinelli E, et al. Solid-state gas sensors for breath analysis: a review. Anal Chim Acta, 2014, 824, 1
[39] Gao M R, Xu Y F, Jiang J, et al. Nanostructured metal chalcogenides: synthesis, modification, and applications in energy conversion and storage devices. Chem Soc Rev, 2013, 42, 2986
[40] Burda C, Chen X B, Narayanan R, et al. Chemistry and properties of nanocrystals of different shapes. Chem Rev, 2005, 105, 1025
[41] Lai C H, Lu M Y, Chen L J. Metal sulfide nanostructures: synthesis, properties and applications in energy conversion and storage. J Mater Chem, 2012, 22, 19
[42] Liu R, Duay J, Lee S B. Heterogeneous nanostructured electrode materials for electrochemical energy storage. Chem Commun, 2011, 47, 1384
[43] Galileo S, Kaushik R C, Jegadesan S, et al. Organic and inorganic blocking layers for solution-processed colloidal PbSe nanocrystal infrared photodetectors. Adv Funct Mater, 2011, 21, 167
[44] Amol S, Li X, Vladimir P, et al. Polarization-sensitive nanowire photodetectors based on solution-synthesized CdSe quantum-wire solids. Nano Lett, 2007, 7(10), 2999
[45] James W G, Katherine L R, Zhang J, et al. Synthesis and characterization of Au/Bi core/shell nanocrystals: a precursor toward II–VI nanowires. J Phys Chem B, 2004, 108, 9745
[46] Supriya A P, Hwang Y T, Vijaykumar V J, et al. Solution processed growth and photoelectrochemistry of Bi_2S_3 nanorods thin film. J Photochem Photobiol A, 2017, 332, 174
[47] Sean K, Emmanuel L, Vuk B, et al. Mid-infrared HgTe colloidal QDs photodetectors. Nat Photonics, 2011, 5, 489
[48] Jung H Y, Jin J, Hyun M P, et al. Synthesis of quantum-sized cubic ZnS nanorods by the oriented attachment mechanism. J Am Chem Soc, 2005, 127, 5662
[49] Byron G, Wu Y, Yin Y, et al. Single-crystalline Nanowires of Ag_2Se can be synthesized by templating against nanowires of trigonal Se. J Am Chem Soc, 2001, 123, 11500
[50] Manish C, Hyeon S S, Goki E, et al. The chemistry of two-dimensional layered transition metal dichalcogenide nanosheets. Nat Chem, 2013, 5, 263
[51] Huang X, Zeng Z, Zhang H. Metal dichalcogenide nanosheets: preparation, properties and applications. Chem Soc Rev, 2013, 42, 1934
[52] Wang Q H, Kourosh K Z, Andras K, et al. Electronics and optoelectronics of two-dimensional transition metal dichalcogenides. Nat Nanotechnol, 2012, 7, 699
[53] Xu M, Tao L, Shi M, et al. Graphene-like two-dimensional materials. Chem Rev, 2013, 113, 3766
[54] Valeria N, Manish C, Mercouri G K, et al. Liquid exfoliation of layered materials. Science, 2013, 340, 1226419
[55] Sun Y, Gao S, Xie Y. Atomically-thick two-dimensional crystals: electronic structure regulation and energy device construction. Chem Soc Rev, 2014, 43, 530
[56] Li H, Wu J, Yin Z, et al. Preparation and applications of mechanically exfoliated single-layer and multilayer MoS_2 and WSe_2 nanosheets. Acc Chem Res, 2014, 47, 1067
[57] Marseglia E A. Transition metal dichalcogenides and their intercalates. Int Rev Phys Chem, 1983, 3, 177
[58] Wilson J A, Yoffe A D. The transition metal dichalcogenides discussion and interpretation of the observed optical. electrical and structural properties. Adv Phys, 1969, 18, 193
[59] Jonathan N C, Mustafa L, O'Neill A, et al. Two-dimensional nanosheets produced by liquid exfoliation of layered materials. Science, 2011, 331, 568
[60] Seo J W, Jun Y W, Park S W, et al. Two-dimensional nanosheet crystals. Angewandte Chemie International Edition, 2007, 46, 8828
[61] Zhang J, Boris D C, Ryan W C, et al. Preparation of Cd/Pb chalcogenide heterostructured janus particles via controllable cation exchange. ACS Nano, 2015, 9, 7151
[62] Dai X, Zhang Z, Jin Y, et al. Solution-processed, high-performance light-emitting diodes based on QDs. Nature, 2014, 515, 96
[63] Liu Z, Peng S, Xie Q, et al. Large-scale synthesis of ultralong Bi_2S_3 nanoribbons via a solvothermal process. Adv Mater, 2003, 15, 936
[64] Yao W T, Yu S H, Wu Q S. From mesostructured wurtzite ZnS-nanowire/amine nanocomposites to ZnS nanowires exhibiting quantum size effects: a mild-solution chemistry approach. Adv Funct Mater, 2007, 17, 623
[65] Dong H, Steven M H, Yin Y, et al. Cation exchange reactions in ionic nanocrystals. Science, 2004, 306, 1009
[66] Vanitha P V, O'Brien P. Phase control in the synthesis of magnetic iron sulfide nanocrystals from a cubane-type Fe–S cluster. J Am Chem Soc, 2008, 130, 17256
[67] Liu H, Tang J, Illan J K, et al. Electron acceptor materials engineering in colloidal QDs solar cells. Adv Mater, 2011, 23, 3832
[68] Yao K, Gong W W, Hu Y F, et al. Individual Bi_2S_3 nanowire-based room-temperature H_2 sensor. J Phys Chem, 2008, 112, 8721
[69] Cihan K, Chulmin C, Alireza K, et al. MoS_2 nanosheet–Pd nanoparticle composite for highly sensitive room temperature detection of hydrogen. Adv Sci, 2015, 2, 1500004
[70] Steven A M, Gerasimos K, Zhang S, et al. Solution-processed PbS QDs infrared photodetectors and photovoltaics. Nat Mater, 2005, 4, 138
[71] Kangho L, Riley G, Niall M, et al. High-performance sensors based on molybdenum disulfide thin films. Adv Mater, 2013, 25, 6699
[72] Dhawale D S, Dubal D P, Jamadade V S, et al. Room temperature LPG sensor based on n-CdS/p-polyaniline heterojunction. Sens Actuators B, 2010, 145, 205
[73] Song Z, Huang Z, Liu J, et al. Fully stretchable and humidity-resistant QDs gas sensors. ACS Sens, 2018, 3, 1048
[74] Li M, Zhou D, Zhao J, et al. Resistive gas sensors based on colloidal QDs (CQD) solids for hydrogen sulfide detection. Sens Actuators B, 2015, 217, 198
[75] Zhu L, Feng C, Li F, et al. Excellent gas sensing and optical properties of single-crystalline cadmium sulfide nanowires. RSC Adv, 2014, 4, 61691